macromol

MDPI

Review

Advances in Alkylated Chitosan and Its Applications for Hemostasis

Huiyang Jin and Zhengke Wang *

MOE Key Laboratory of Macromolecular Synthesis and Functionalization, Department of Polymer Science and Engineering, Zhejiang University, Hangzhou 310027, China; 3170105780@zju.edu.cn

* Correspondence: wangzk@zju.edu.cn

Abstract: Chitosan, a natural polysaccharide, has been widely used as a biomaterial, especially for hemostasis. However, hemostatic materials processed from pure chitosan have limited hemostatic effect and are extremely unstable in some cases; chemical modification is therefore needed to improve the hemostatic properties of chitosan. Through chemical reactions with hydroxyl and amino groups in chitosan macromolecules, such as alkylation, carboxylation, quaternization, etc., different groups can be introduced into the repeating units. Moreover, the introduction of different substituents can endow chitosan with more functions. For example, the introduction of long alkyl chains can improve its hydrophobic property, and greatly improve its hemostatic property. However, there is still no review of alkylated chitosan for hemostasis. Therefore, we introduce in detail several methods (direct alkylation, reductive alkylation and acylation reaction) for preparing alkylated chitosan and its applications for hemostasis.

Keywords: chitosan; alkylation; hemostasis; alkylated chitosan; biomaterial; polysaccharide

Citation: Jin, H.; Wang, Z. Advances in Alkylated Chitosan and Its Applications for Hemostasis. *Macromol* **2022**, *2*, 346–360. https://doi.org/10.3390/macromol2030022

Academic Editor: Dimitrios Bikiaris

Received: 8 June 2022
Accepted: 23 July 2022
Published: 27 July 2022

1. Introduction

Massive bleeding often leads to death, so it is essential to develop dressings with strong hemostatic effect. Natural macromolecules, such as gelatin, alginate, oxidized cellulose, chitosan, etc., are often used as hemostatic materials.

Gelatin and collagen have a very strong coagulation ability, but some individuals have immune reactions, so the actual production should be strictly controlled. Alginate hemostatic materials have poor adhesion, which can prevent secondary damage. Oxidized cellulose is acidic, enabling platelet activation and aggregation to stop bleeding, but it can also cause inflammation of surrounding tissues [1], and damage the nervous system when the carboxyl content is too high [2].

Chitosan is a linear, semi-crystalline natural polysaccharide, composed of the repeating units N-acetylglucosamine and glucosamine residues. It is partially deacetylated from chitin, which is one of the most abundant carbohydrates in nature [3–5]. It has excellent biological properties, such as biocompatibility, biodegradability, mucosal adhesion, and so on [6–10]. It also has anti-tumor, antioxidant and antibacterial properties. Therefore, chitosan and its derivatives are widely used in biomaterials [11–14], food preservation [15,16], cosmetics [17–19], water treatment [20,21], and textile engineering [22,23]. However, chitosan also has some disadvantages. For example, its effect on severe bleeding is limited and extremely unstable in some cases [24]. Therefore, its hemostatic properties should be improved by chemical modification.

There are hydroxyl and amino groups in chitosan macromolecules. Through chemical reaction, such as alkylation, carboxylation, and quaternization [25], different groups can be introduced into the repeating units. Moreover, the introduction of different substituents can endow chitosan with more functions (Table 1). For example, the introduction of long alkyl chain can improve its hydrophobic properties, increase its solubility in organic solvents, and greatly improve the hemostatic of chitosan. Alkylated chitosan can be synthesized by

reductive alkylation, acylation and other methods, and the degree of substitution (DS) can be adjusted by changing the proportion of raw materials to give alkylated chitosan more different properties. However, there is still no review of alkylated chitosan. Therefore, we introduced in detail several methods for preparing alkylated chitosan and its applications for hemostasis.

Table 1. Different kinds of chitosan derivatives and their synthetic methods, physical properties and applications.

Chitosan Derivatives	Synthesis	Physical Properties	Applications
Alkylated chitosan	with Aldehyde with Haloalkane Acylation	Amphiphilicity	Hemostasis Antibacterial [26]
Carboxymethyl chitosan [27]	Schiff base reaction	Hydrophilicity pH responsiveness	Cosmetic Drug delivery Miscellaneous
Quaternary ammonium salts of chitosan [28]	Directly quaternary ammonium at the amine units Side chain quaternary ammonium	Water solubility Positive charge	Gene therapy Drug delivery Wound healing Tissue engineering
NIPAAm-chitosan [29]	Acylation	Temperature sensitivity	DNA delivery

2. Synthesis of Alkylated Chitosan

2.1. Reductive Alkylation by Using Aldehyde

Alkylated chitosan with aldehyde was produced via the following procedure [30]: firstly, chitosan was completely dissolved in acetic acid aqueous solution, and then different volumes of aldehyde were added. The nitrogen atom with lone pair electrons in the primary amino group of chitosan attacks the positively charged carbon atom in the aldehyde group, and removes a molecule of H_2O to obtain the Schiff base structure. Then, the sodium borohydride alkaline solution is added to reduce the unstable C=N double bond, so as to form a stable CN single bond. After stirring the mixture for 12 h at 25 °C, the pH was adjusted to 5 and $NaBH_4$ was added. Before adjusting pH to 7, the mixture was stirred for 3 h. Then the precipitate was washed with ethanol, and the product was freeze-dried (Figure 1a).

Petit et al. [31] produced alkylated chitosan by using aldehyde via microwave irradiation. In order to choose a more suitable microwave heating method, pulsed power mode (SPS) and dynamic mode (DYN) are compared. DYN mode was defined by a high initial microwave power and reached the set reaction temperature in less than ten seconds. Once the target temperature was reached, the microwave power dropped or was turned off completely to maintain it. Therefore, most reactions were carried out at very low or no microwave radiation. The SPS mode allowed the irradiation power to change the target reaction temperature. The reaction mixture was irradiated with the set power to maintain the target temperature. The irradiation time of SPS is longer and the irradiation power is more stable. Lastly, the temperature distribution of the SPS reaction process was compared with that of conventional heating (i.e., water bath heating). Even when the irradiation power was as low as 30 W, it took about 100 s to reach 40 °C under microwave irradiation, while it took almost 600 s in preheated water bath to achieve the same effect. The yield under microwave radiation was higher than that under conventional heating, and its specific value was related to temperature, raw material ratio and reaction time. For example, when the raw material ratio with 10% alkylation as the target was heated at 25 °C for 1 h, the yield of conventional heating was 63%, while that of microwave heating was 72%. Microwave radiation might realize "green chemistry" from the perspective of energy.

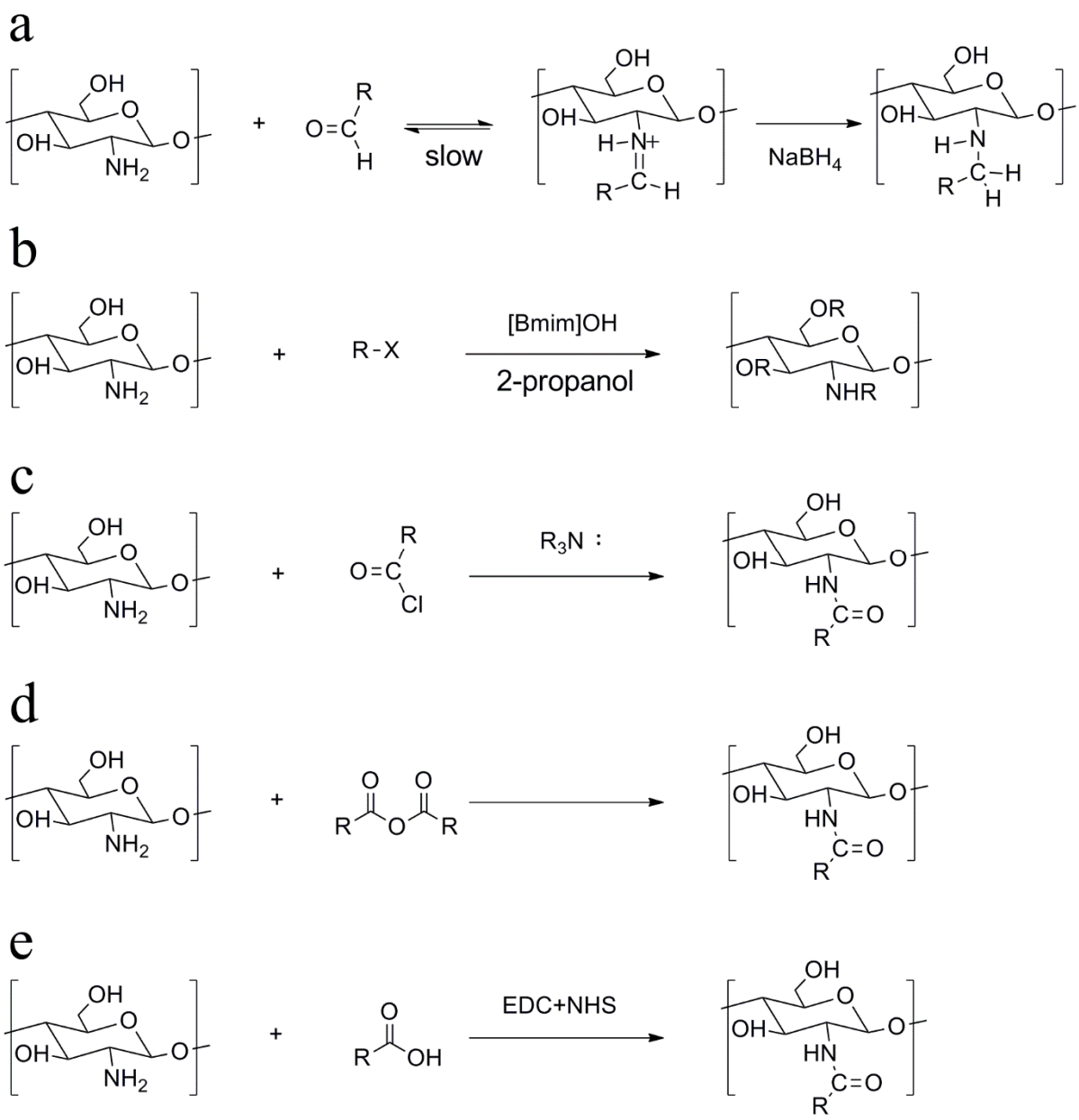

Figure 1. Scheme of alkylated chitosan through different chemical reactions: (**a**) reductive alkylation, (**b**) alkylation through haloalkanes and amino reaction, (**c**) alkylation with acyl chlorides, (**d**) alkylation with anhydrides and (**e**) alkylation with fatty acids.

2.2. Alkylation through Haloalkanes and Amino Reaction

Alkali/urea aqueous solution as a new type of solvent was developed to directly dissolve chitosan at a low temperature, which is a more sustainable alternative than acidic solvent [32–34]. It has been proved that chitosan was mainly dissolved by breaking the original hydrogen bonds in the alkaline solution [35,36]. Sun et al. attached bromohexane, bromododecane and bromooctadecane to the amino group of chitosan, respectively [37]. The specific synthesis method is as follows: chitosan was first dissolved in acetic acid solution and then neutralized with NaOH solution. After separating the white chitosan flocs, NaOH solution was added to adjust pH = 9. It was settled overnight, rinsed with deionized water 1 or 2 times and freeze-dried. The purified chitosan was dissolved in an alkaline solution at -20 °C with a KOH/urea/water ratio of 16/8/76 and stored at 4 °C for future use. The haloalkane and chitosan solutions were mixed in a molar ratio of 3:1, and

the reaction mixture was stirred for 12 h at 25 °C; the product was then neutralized with 50% (*v*/*v*) HCl, dialyzed with distilled water and freeze-dried.

In order to make the reaction more environmentally friendly, Pei et al. reported a novel method to synthesize alkylated chitosan with 1-butyl-3-methylimidazolium hydroxide [Bmim]OH basic ionic liquid as an alkaline reagent [38]. Chitosan was added in 2-propanol at room temperature and the mixture was stirred. [Bmim]OH was then added. The mixture was heated to 40 °C and alkalized under stirring for 1 h before haloalkanes (bromoethane, 1-chlorobutane, bromododecane, or bromohexadecane) were added. The mixture was heated to 80–100 °C and reacted at this temperature for 8–10 h. After the reaction, the reactants were filtered, and the filter residue was washed with ethanol and anhydrous dichloromethane in turn, and dried at 50 °C. The effects of alkalizing agents such as NaOH, [Bmim]OH and [Bmim]Cl on the DS of alkylated chitosan were compared. When [Bmim]OH was used as an alkalizing reagent, the DS value of dodecyl chitosan was the largest (58.4%), while that of using NaOH was 48.5%, and that of using [Bmim]Cl was 15.9%. The reusability of the ionic liquid was also investigated, and the experimental results indicated that there was no noticeable change in the DS of the alkylated chitosan after the ionic liquid was used three times (Figure 1b).

2.3. Alkylation by Acylation Reaction

Le Tien et al. processed acylated chitosan using palmitoyl chloride, caproyl chloride, octanoyl chloride and myristoyl chloride [39]. Chitosan was added to the acetic acid aqueous solution, and the mixture was fully stirred. Then, NaOH was slowly added under strong stirring to adjust the pH to 7.2. Acyl chloride was then added, and the mixture was diluted with distilled water. After a period of time, the mixture was neutralized, precipitated with acetone, washed with methanol, and dried.

Rodrigues prepared acylated chitosan using stearoyl and lauroyl chloride (Figure 1c) [40]. Chitosan was dissolved in the acetic acid aqueous solution, and triethylamine and the acyl chloride were added, under continuous stirring at 18 °C for 1 h. The mixture was precipitated in ethanol, filtered, and washed with ethanol and hexane. The product was extracted with hexane to ensure the elimination of unbound acyl chloride. The DS was controlled by the acyl chloride amount.

Anhydride can also be used to prepare acylated chitosan. Hu et al. prepared acylated chitosan with acetic anhydride, propionic anhydride and hexanoic anhydride (Figure 1d) [41]. Chitosan was dissolved in the acetic acid aqueous solution; the anhydrides ethanol solution was added slowly with stirring. After continuous stirring for 4 h, the reaction solution was neutralized. Finally, the products were washed with water and ethanol repeatedly and dried under vacuum.

Zhang et al. used lauric anhydride to prepare O-acylated chitosan nanofibers [42]. Chitosan nanofibers were dispersed in a premixed solution of pyridine and lauric anhydride. The mixture was gently stirred at 50 rpm for 2 h at 80 °C. After acylation, the nanofibers were washed repeatedly with excess distilled water and methanol to remove unreacted reagents and hydrolyze trifluoroacetate. The nanofibers were then freeze-dried. Because trifluoroacetic acid added during the formation of chitosan nanofibers has a protective effect on the amino group, the acylation reaction was carried out only on the hydroxyl group.

Wang et al. used capric acid to synthesize acylated chitosan (Figure 1e) [43]. Chitosan was dissolved in the acetic acid aqueous solution, and the mixture was fully stirred until the chitosan was completely dissolved. The capric acid was dissolved in anhydrous ethanol and then EDC (1-(3-dimethylaminopropyl)-3-ethylcarbodiimide hydrochloride) and NHS (N-hydroxy succinimide) were added under continuous stirring to activate carboxyl groups on the fatty acid. The acid solution was added dropwise into the chitosan solution and reacted under stirring for a period of time, and then anhydrous ethanol was added into the reaction solution to precipitate the product. Finally, the product was obtained by centrifugation, washed with ethanol, and dried.

3. Applications of Alkylated Chitosan for Hemostasis

3.1. Hemostatic Mechanism of Alkylated Chitosan and Effect of Molecular Structure on Hemostatic Properties

Chen et al. obtained alkylated chitosan with a different graft chain length by reacting hexanal aldehyde, dodecanal aldehyde and octadecyl aldehyde with chitosan [30]. The hemolysis rate of all samples was less than 5%, and there was no significant difference between chitosan and alkylated chitosan. When the DS is the same, the longer the alkyl chain, the better the coagulation performance. And the smaller the DS when using the same aldehyde, the more obvious the coagulation performance. Activated partial thromboplastin time (APTT) is generally considered to be an effective method to evaluate the endogenous coagulation system. Prothrombin time (PT) is the most sensitive and commonly used screening test, which mainly reflects the exogenous coagulation state. Thrombin time (TT) is used to measure the ability of fibrinogen to form fibrin (common pathway). The difference in the APTT, PT and TT results of each material was very small, which shows that alkylated chitosan hemostasis does not play a role through traditional endogenous, exogenous and common ways. Therefore, they predicted that thrombosis is caused by the action of alkylated chitosan on platelets and red blood cells. Chitosan and each alkylated chitosan can adhere, deform and aggregate a large number of cells, indicating their excellent efficiency in stimulating and activating platelets. However, the number of normal and deformed platelets adhered to chitosan was almost the same as that on alkylated chitosan. Alkylated chitosan did not cause a significant increase in intracellular Ca^{2+} concentration, nor could it promote the release of CD62p, which indicated that alkylated chitosan did not significantly improve platelet adhesion and aggregation; Liu et al. obtained similar results [44]. The number of red blood cells adsorbed by alkylated chitosan was significantly higher than that of chitosan, and the number of active red blood cells increased significantly with the increase in the carbon chain length of grafted alkanes (Figure 2). Combined with the results of the platelet analysis, they concluded that the acceleration in blood coagulation may be related to the effect of the alkylated chitosan on red blood cells rather than platelets. Their hypothesis of the alkylated chitosan coagulation process is shown in Figure 3. When the blood contacts with alkylated chitosan, all elements in the blood work together in chronological order through traditional ways until the fibrinogen is decomposed into fibrin, and then forms a fibrin network. At the same time, the alkylated chitosan can promote the activation and aggregation of platelets and red blood cells. On this basis, the preliminary packaging of materials and blood cells can be developed. In this process, the length of the alkyl carbon chain in the alkylated chitosan affects its activation of erythrocytes. The carbon chain of alkyl in the alkylated chitosan is longer, which makes more red blood cells adhere and aggregate, so more red blood cells can be fixed in the package. Finally, the previous alkylated chitosan platelet erythrocyte package may be combined with fibrin polymer to form a thrombus. In this way, the alkylated chitosan, especially those with long-chain alkane groups, may significantly promote thrombosis.

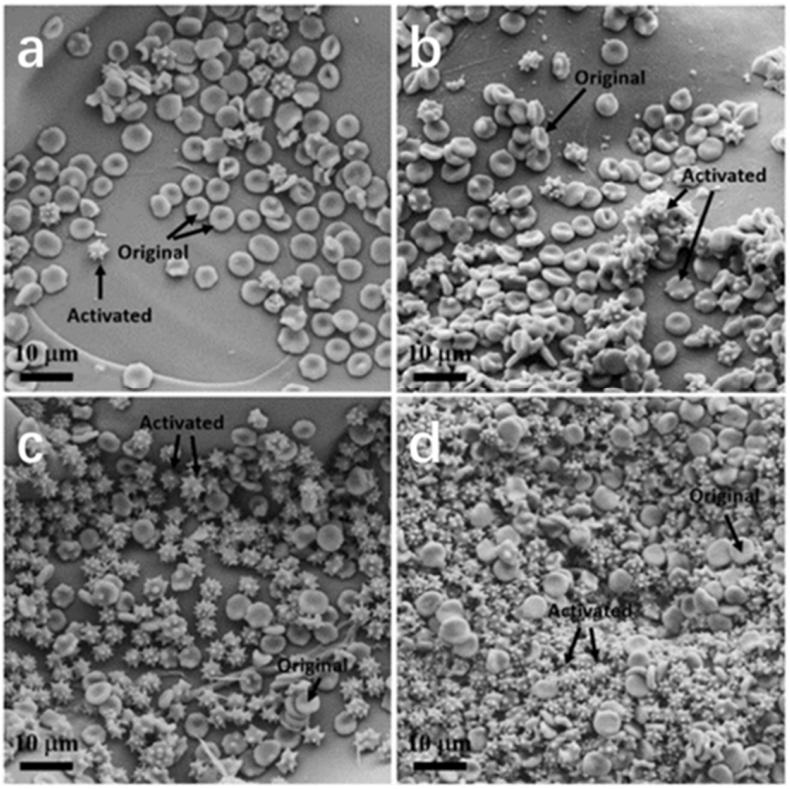

Figure 2. SEM images of erythrocyte adhesion on (**a**) chitosan, (**b**) chitosan (6C), (**c**) chitosan (12C), and (**d**) chitosan (18C) [30].

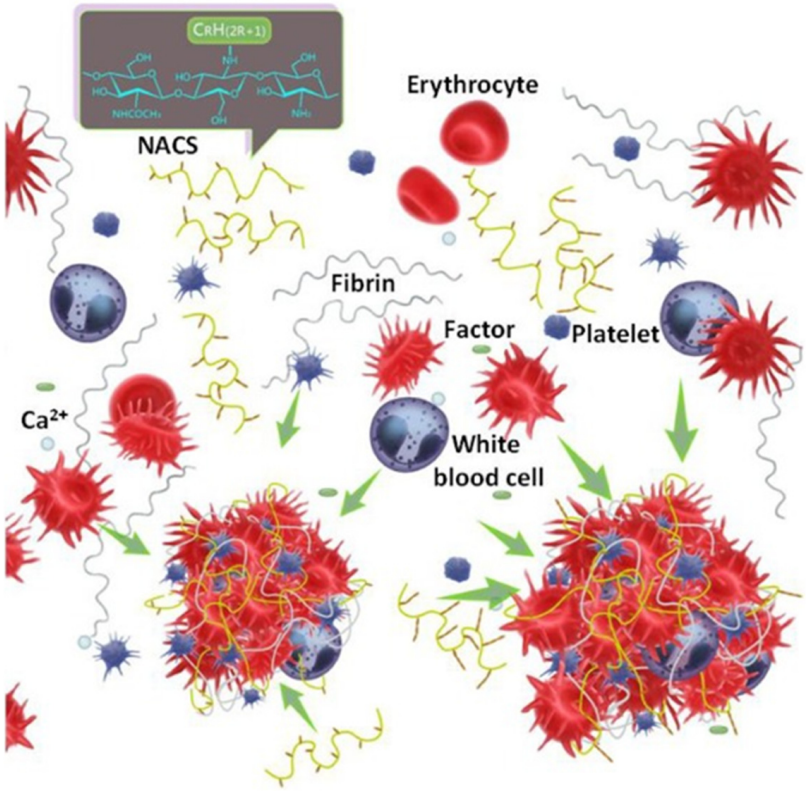

Figure 3. Coagulation process involving alkylated chitosan [30].

As mentioned above, Chen et al. believed that modified chitosan did not affect the path of endogenous coagulation and ordinary blood coagulation, which was somewhat different from the conclusion of Huang et al. [45]. Huang et al. prepared hydrophobic chitosan with different grafting rates (0.24, 2.1, 5.1 and 8.4%) from lauraldehyde and chitosan. Compared with unmodified chitosan samples, the APTT value of modified samples was higher and greater than that of PBS samples, which indicates that hydrophobic chitosan affects the path of endogenous coagulation and ordinary blood coagulation, and prolongs the time of fibrin blood clot formation; that is, chitosan and hydrophobic chitosan can affect the activity of plasma coagulation factors. One explanation is that cationic polymers and negatively charged plasma proteins are attracted by static electricity, which changes the structure of the protein. The APTT value of the hydrophobic chitosan sample was higher than that of the blank control group, but increasing the concentration of hydrophobic chitosan had no significant effect on the APTT value. However, when the hydrophobic chitosan concentration increased, the PT value increased significantly. The electrostatic and hydrophobic forces of hydrophobic chitosan molecules in solution and the electrostatic force of chitosan molecules in solution affect the structure of the fibrinogen and change its function in the coagulation system. The FT value is less affected by hydrophobic chitosan concentration. Compared with the PBS control group, chitosan and hydrophobic chitosan groups prolonged FT time. Thromboelastographic (TEG) assays showed that chitosan affected the coagulation process of autologous blood, prolonged the time required to form fibrin, and reduced the cross-linking speed of fibrin. However, the formation time of fibrin and thrombus in the alkylated chitosan group was significantly shortened, and the higher the grafting rate was, the more obvious the shortening was. In general, chitosan and hydrophobic chitosan have negative effects on endogenous and common blood coagulation pathways.

Huang et al. obtained amphiphilic alkylated chitosan by reacting lauraldehyde with chitosan, which can convert whole blood into gel [46]. As for the hemostatic mechanism, they speculated that the hydrophobic long chain of the alkylated chitosan is anchored to form a 3D network on red blood cells. Chen et al. found that the number of normal and deformed platelets adhered to the chitosan is almost the same as that on alkylated chitosan. Wang et al. reported that most platelets in the chitosan group were non-activated [47]. In the chitosan(6C), chitosan(12C) and chitosan(18C) nanofiber membrane groups, most platelets adhered to nanofibers showed activation because they almost all stretched irregularly and formed pseudo-feet. The self-assembly of the hydrophobically modified chitosan chain hydrophobically anchored on the blood cell membrane, so as to bridge the cells into a 3D network. In addition, due to the nano size, voids and curls in alkylated fibers, fibrin networks and nanofiber networks intercept platelets in a similar way. The thrombus fibrin and thrombus formation time of the alkylated chitosan group decreased significantly, and chitosan(18C) decreased the most, indicating that it had the most significant coagulation properties in vitro.

3.2. Different Forms of Alkylated Chitosan Hemostatic Materials

Dowling et al. synthesized hydrophobic chitosan by attaching benzene-n-octadecyl tails to the chitosan backbone via a reaction with 4-octadecylbenzaldehyde [48]. They evaluated the hemostatic properties of the alkylated chitosan solution with animal injury models. First, they assessed the damage to a small animal. Femoral vein injury was caused in Long–Evans adult rats by scalpel, and then the solution (0.5 wt% alkylated chitosan solution, saline buffer, and 0.5 wt% chitosan solution) was applied to the wound through a syringe. The hemostatic time of the alkylated chitosan solution was 5.6 s, while those of the normal saline and chitosan solutions were 50 s and 47 s, respectively. Next, they evaluated alkylated chitosan bandages for the treatment of high pulsatile injury in the pig femoral artery injury model. In this model, the femoral artery was severed, and free bled, which could be fatal within 15 min without treatment. The alkylated chitosan bandage was able

to stop bleeding after 2 min of compression. When the bandage was removed after 3 h, the arterial injury was successfully coagulated, and all the pigs survived the experiment.

Alkylated chitosan could transform whole liquid blood into gel, which could quickly stop bleeding from both minor and severe injuries in small and large animals. The mechanism of gelation was based on self-assembly of the alkylated chitosan chain. The self-assembly method made their hydrophobicity anchored in the blood cell membrane, so as to connect the cells into a three-dimensional network. Therefore, these cells were active components (nodes or junction points) in the network, rather than physically trapped in the polymer network. As shown in Figure 4, the polymer is shown schematically with its hydrophilic backbone in blue and the grafted benzyloctadecyl hydrophobes in purple. When added into the liquid blood, the components assemble into a three-dimensional network (gel), as shown on the right. This is driven by the insertion of hydrophobes into blood cell membranes (as depicted in the top inset); thereby the polymer chains connect (bridge) the cells into a self-supporting network. The gelling ability of alkylated chitosan was similar to that of the fibrin-based sealant, but the cost was much lower. Another important aspect of alkylated chitosan as a hemostatic agent was that its gelling effect on blood could be reversed by adding supramolecular α-cyclodextrin (α-CD) by isolating hydrophobic molecules and preventing them from attaching to blood cells.

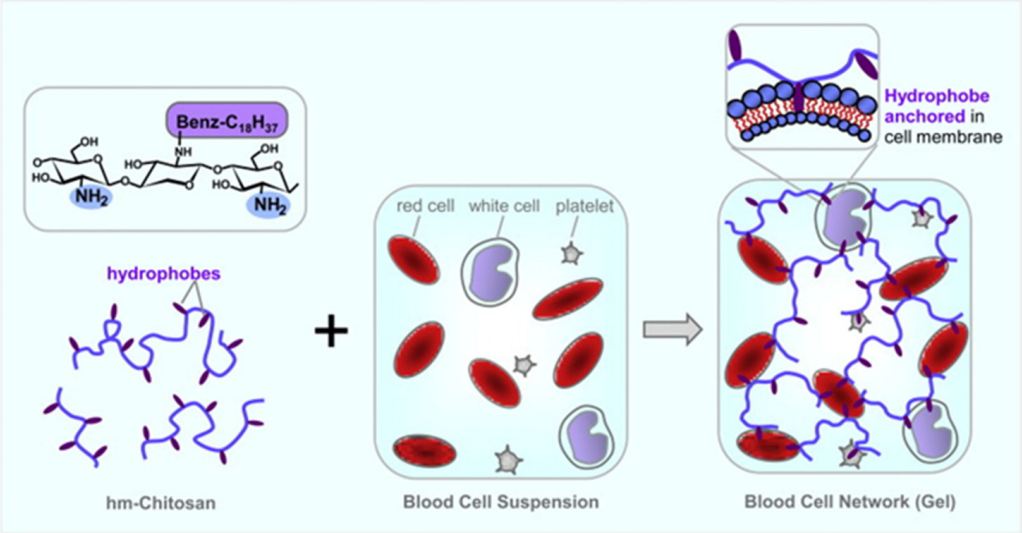

Figure 4. Mechanism for gelation of blood by alkylated chitosan [49].

Alkylated chitosan foam could also be used as a hemostatic adjunct or solitary hemostatic intervention [49]. Alkylated chitosan foam showed no significant toxicity, and immobilized blood cells into clusters between adjacent bubbles in the foams, while the chitosan controls did not immobilize the blood cells. And the alkylated chitosan concentrates can be packaged and sprayed as expanding foams. In the severe liver injury model, spraying alkylated chitosan foam directly on the damaged liver surface could significantly reduce the blood loss, and improve the survival rate. Alkylated chitosan was obtained by reacting chitosan with dodecaldehyde or 4-octadecylbenzaldehyde through reductive alkylation, and the DS was 1%, 2.5% and 5%. They performed non-lethal hepatectomy tests on rats for each hydrophobic chitosan formulation, and added unmodified chitosan control group and no treatment control group (NT). In order to cause injury and bleeding, a segment of the medial lobe of the liver, representing 14 ± 3% of the initial liver weight, was removed with surgical scissors. This injury was fatal, and the average survival time was 17.2 ± 0.84 min. When the carbon canister is activated, the foam can be easily applied to the body cavity. The survival rates of NT and chitosan control groups were 0%. In sharp contrast, the survival rate of all injuries treated with alkylated chitosan improved, and reached 100% within 60 min.

Alkylated chitosan foam synthesized by grafting N-palmitoyl tail onto the chitosan chain through the reaction with palmitic anhydride, and the animal experiments were divided into four groups: NT, chitosan, alkylated chitosan, a fibrin-based agent-TISSL (FS) [50]. After the liver injury, all hemostatic agents successfully induced thrombosis, and the hemostatic foam was able to repair the liver injury. Six weeks after treatment, the residual FS showed obvious adhesion between the liver injury site and the surrounding tissue. In contrast, slight adhesion was observed in the chitosan and alkylated chitosan groups. Histopathology of the alkylated chitosan group showed a tissue repair phenotype similar to that of the control group, which was different from the other two hemostatic agents.

In addition, they also compared the therapeutic effects of an alkylated chitosan gauze, a chitosan gauze and a combat gauze on the model of fatal bleeding in sows [51]. Chitosan was modified by n-decanal. The two chitosan-based gauzes are more viscous than the combat gauze. In addition, the tissue adhesion of the alkylated chitosan gauze was significantly higher than that of the chitosan gauze (15.3 $\pm$ 4.2 kPa vs. 8.4 $\pm$ 3.5 kPa). During the treatment, there was no significant difference in the overall survival time, hemostasis duration and the number of dressings used in each experimental group, but the blood loss after treatment in the hm-c gauze group was significantly lower than that in other treatment groups. All animals in the alkylated chitosan gauze treatment group survived, while only three of the four animals in the combat gauze and chitosan gauze control groups survived.

In order to integrate the microchannel structure into a chitosan sponge, Du et al. designed hemostatic microchannel alkylated chitosan sponges (MACSs) with different porosity and highly interconnected microchannels by combining 3D printing microfiber leaching, freeze-drying and surface activity modification, as shown in Figure 5 [26]. The DS of the dodecanal was 27.86 $\pm$ 18.99%. There was a layered porous structure in the MACS, including microchannels and micropores, while only micropores were randomly distributed in the whole alkylated chitosan. With the increase in the polylactic acid (PLA) microfiber filling rate, the porosity of the MACSs gradually increased from 73.2 $\pm$ 2.9% to 88.8 $\pm$ 1.6%, which was significantly higher than 32.1 $\pm$ 1.9% of the alkylated chitosan. When the chitosan concentration was lower than 4%, the sponge could not maintain its shape. Chitosan solution with concentration higher than 4% had high viscosity, and it is difficult to inhale the gap in the PLA microfiber template under negative pressure. Therefore, 4% chitosan solution was selected to prepare the MACS. The filling rate of the PLA microfiber template increased from 20% to 60%, and the compressive stress decreased from 46.2 $\pm$ 8.0 to 8.1 $\pm$ 0.9 kPa. The MACS sponge had strong mechanical strength after blood suction. Compared with the alkylated chitosan, the MACS had higher mechanical strengthening folding. In addition, the mechanical strengthening fold of the MACS gradually increased with the increase in porosity. This is because MACSs with high porosity and a large specific surface area can absorb more blood, promote full contact between blood and the matrix and form more blood clots. The MACS had the lowest BCI value compared with gauze, gelatin sponge and celox used clinically™, CELOX™-G, alkylated chitosan and microchannel chitosan by the in vitro coagulation experiment. The MACS also has stronger procoagulant and hemostatic ability in the lethal normal and heparinized rat- and pig-liver perforation wound models.

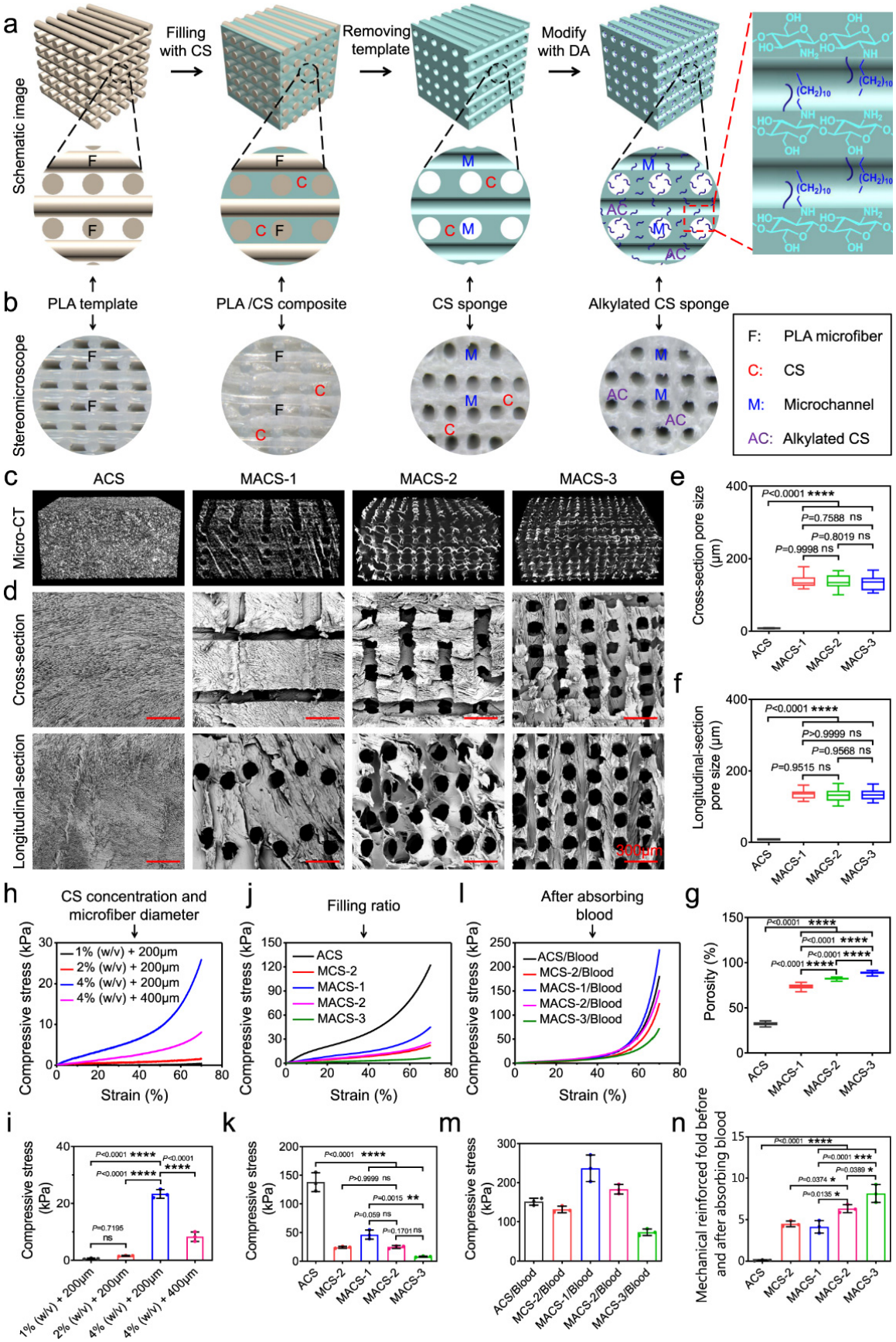

Figure 5. Fabrication and characterization of the MACS with different porosity. (**a**) Schematic illustration

of the fabrication process of the MACSs; (**b**) Stereomicroscopic images of the PLA microfiber template, PLA composite, micro channeled chitosan sponge, and micro channeled alkylated chitosan sponge; (**c**,**d**) Micro-CT and SEM images showing the macro and microstructure of the akylated chitosan and MACS-1/2/3 (the filling ratios of PLA microfiber template is 20, 40, or 60%); (**e**) The pore size of the alkylated chitosan and MACS-1/2/3 in cross-section and longitudinal-section (pore size, n = 16); (**f**) The pore size of the alkylated chitosan and MACS-1/2/3 in longitudinal-section (pore size, n = 16); (**g**) The porosity of the alkylated chitosan and MACS-1/2/3 (porosity, n = 25); (**h**,**i**) Compressive stress-strain curves and compressive stress of the MACSs with different CS concentrations (1, 2, and 4% (*w/v*)) and PLA microfiber diameter (200 and 400 μm) (n = 3 independent samples); (**j**–**m**) Compressive stress-strain curves and compressive stress of the alkylated chitosan, MCS-2, and MACS-1/2/3 before and after absorbing blood; (**n**) Mechanically reinforced folds of the alkylated chitosan, MCS-2, and MACS-1/2/3 before and after absorbing blood (n = 3 independent samples). Data are expressed as mean ± SD. The significant difference was detected by one-way ANOVA with Tukey's multiple comparisons test. The "ns" indicated no significant difference, * $p < 0.05$, ** $p < 0.01$, *** $p < 0.001$, **** $p < 0.0001$ [26].

3.3. Alkylated Chitosan Hemostatic Material Compounded with Other Materials

To improve the hemostatic properties of alkylated chitosan, researchers combined it with other materials. Based on the positive charge of chitosan and the negative charge of mesoporous silica nanoparticles (MSNs), Chen et al. combined alkylated chitosan and MSNs to develop a rapid hemostatic agent with the advantages of both materials and minimal side effects [52]. Alkylated chitosan was obtained by alkylation of chitosan and 4-octadecylbenzaldehyde, and the DS is 5%. Alkylated chitosan and MSN were mixed by ultrasonic. In order to improve the hydrophilicity of the material, glycerol (G) was added to produce mesoporous silica nanoparticle-glycerol alkylated chitosan (MSN–GACS). The hemostatic effect was best when the molar ratio of alkylated chitosan: G: MSN was 1:1:0.25, which was better than MSNs and alkylated chitosan. TEG results showed that alkylated chitosan, MSN, MSN–GACS and kaolin (the main component of combat gauze) significantly promoted blood coagulation. Alkylated chitosan performed the worst in the four experimental groups, and MSN–GACS performed the best. After incubation in PRP for 15 minutes, alkylated chitosan and NAC–GACS attracted more platelets than the combat gauze and MSN. By quantifying the adhesion of platelets to each material, it can be found that combat gauze, MSN, alkylated chitosan and MSN–GAC attract more platelets than the control group (standard gauze). At the same time, compared with alkylated chitosan, MSN or the combat gauze, platelets adhered to MSN–GACS increased significantly. In addition, there was no significant difference between MSN and combat gauze during the first 15 minutes of incubation. However, after 30 min, more platelets were observed on MSN than on combat gauze, indicating that MSN showed better hemostatic efficiency than the combat gauze. In addition, compared with alkylated chitosan or MSN, the platelet adhesion of MSN–GACS increased, indicating that MSN–GACS has the best hemostatic efficiency, and its performance is much better than that of the combat gauze. The same conclusion was obtained in the whole blood absorption experiment. Compared with the combat gauze, MSN–GACS can absorb more blood cells in the rabbit femoral artery and liver injury model, induce less cytotoxicity in vitro, and show better hemostatic effect.

In order to improve the mechanical strength of alkylated chitosan and overcome the possible toxicity of graphene oxide (GO), Zhang et al. prepared a series of composite sponge ACGSs with different proportions (GO/alkylated chitosan, 0%, 5%, 10% and 20%) through dilute solution freezing phase separation and drying, in which alkylated chitosan was obtained by the reaction of the dodecanal (the molar feed ratio of the amine group to aldehyde was 1:0.8) [53]. The water absorption and blood absorption capacity of the sponge was higher than that of the gauze, and the water absorption and blood absorption capacity of ACGS20 was higher than that of ACGS0. ACGSs had good blood compatibility (hemolysis <5%) and had no obvious cytotoxicity. ACGSs had the best hemostatic effect in the rabbit femoral injury model, which was better than GO, celox and the gauze. By

evaluating the expression level of CD62p, it was found that the expression level of CD62p in ACGSs increased with the addition of GO; that is, GO could activate platelets (Figure 6).

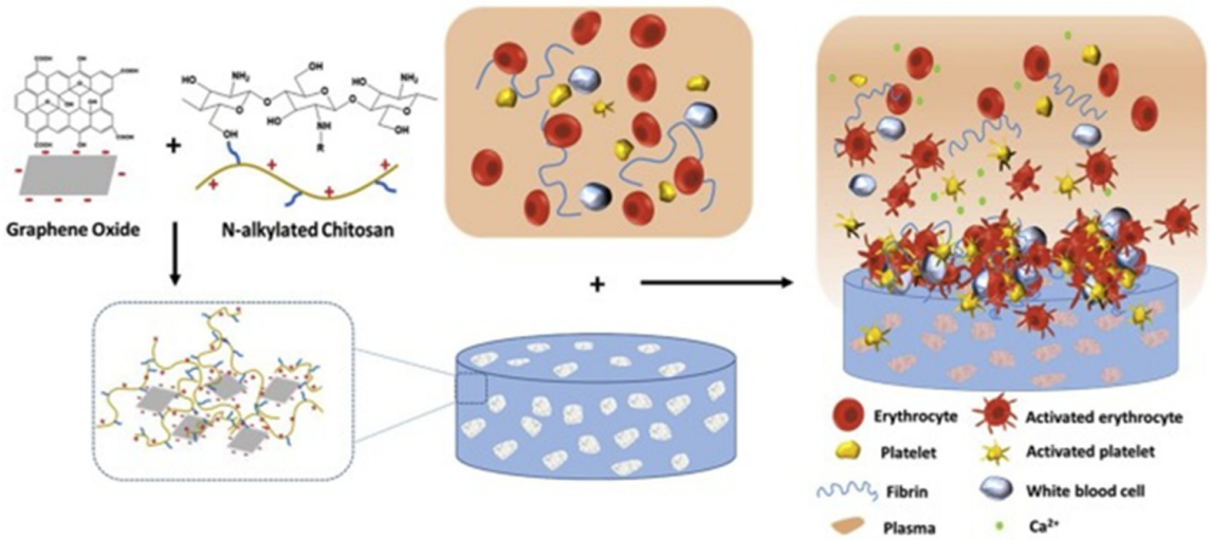

Figure 6. Schematic illustration of alkylated chitosan/GO hemostasis process [53].

Sun et al. prepared alkylated chitosan with different alkyl chain lengths (obtained by the reaction of chitosan with bromohexane, bromodecane or bromooctadecane, and the molar ratio of amino group to bromoalkyl is a 1:0.2, b 1:0.4 and c 1:0.6), and prepared an alkylated chitosan-diatom biomass silicon (AC-DB) sponge by dispersing different concentrations of (0.5%, 1%, *w/v*) diatom biomass silicon (DB) in alkylated chitosan solution [37]. The hemolysis rate of alkylated chitosan grafted with different alkyl groups and different DS was less than 5%. Alkylated chitosan (18C/c) had the best hemostatic effect, so it was selected for further experiments. The BCT of all AC-DB sponges was shortened, the hemostasis time was shorter than alkylated chitosan (18C/c), and the coagulation time was shortened with the increase of DB. In the rat tail transection model, the AC-DB sponge had the best hemostatic effect, the shortest coagulation time (106.2 s) and the lowest blood loss (328.5 mg), while the coagulation time of alkylated chitosan (18C/c) was 199 s, and the blood loss was 989.6 mg. The addition of DB enabled the AC-DB sponge to activate the inherent coagulation pathway, so as to improve the coagulation rate and enhance the intensity of thrombosis. In other words, the addition of DB enabled the AC-DB sponge to activate coagulation factors XI and XII, further effectively activating the endogenous coagulation pathway, and having the ability of rapid coagulation. Moreover, the electrostatic interaction between alkylated chitosan and the DB made the sponge form a three-dimensional network structure with high mechanical strength. Combined with the hydrophobic alkylated chitosan, the internal structure of the composite sponge would be in full contact with the blood to achieve faster hemostasis.

Wang et al. constructed porous sponges (C-ODs) with decanoic acid modified chitosan (CSCA) and oxidized dextran (ODs) [43]. The DS of the CSCA was 33.39%. C-ODs had extremely high hemostatic ability, and that was related to the oxidation degree of the dextran. The higher the oxidation degree, the stronger the hemostatic ability. The hemostatic time of C-ODs applied to mouse tail amputation, rat liver injury and rat leg artery injury models was 325, 185 and 79 s, respectively, which was significantly shorter than that of the gauze (592, 288 and 290 s) and the commercial gelatin sponge (556, 285 and 215 s). C-ODs porous sponges had better hemostatic ability than gauze and commercial gelatin sponges.

4. Conclusions

Chitosan is a non-toxic polycationic polymer. With the in-depth study of chitosan, researchers found that it has weak hydrophobicity and low plasticity. Alkylation can solve this problem to some extent. Alkylated chitosan was synthesized by reductive alkylation, direct alkylation, or acylation reaction. After joining the alkyl chain, the hydrophobicity of chitosan was enhanced, and the hemostatic properties were improved. Moreover, it can be made into composites with other materials to further improve its hemostatic properties.

Alkylated chitosan as hemostatic material still has some problems to be explored, such as the effect of alkylated chitosan on integral activation and the formation time of the thrombus. Chitosan itself has a positive charge; whether the positive charge will be weakened after alkylation, and whether it is related to the length of the graft chain, also need to be further studied. And the synthesis of alkylated chitosan usually uses a lot of organic solvents, which is very unfriendly to the environment and hinders subsequent industrialization. There is, therefore, an urgent need for a greener and non-pollution method to prepare alkylated chitosan. Moreover, many literatures on alkylated chitosan almost tend to discuss its hemostatic effects, and rarely discuss its possible applications in other aspects, which is also an area that needs to be paid more attention to in future research.

Author Contributions: Conceptualization, Z.W.; writing—original draft preparation, H.J.; writing—review and editing, Z.W.; supervision, Z.W.; funding acquisition, Z.W. All authors have read and agreed to the published version of the manuscript.

Funding: This research was funded by National Natural Science Foundation of China, grant number 51873187; Science Fund for Distinguished Young Scholars of Zhejiang Province, grant number LR20E030004; National Basic Research Program of China, grant number 2018YFC1004803.

Institutional Review Board Statement: Not applicable.

Informed Consent Statement: Not applicable.

Data Availability Statement: Not applicable.

Conflicts of Interest: The authors declare no conflict of interest. The funders had no role in the design of the study; in the collection, analyses, or interpretation of data; in the writing of the manuscript, or in the decision to publish the results.

References

1. Fu, L.; Zhang, J.; Yang, G. Present status and applications of bacterial cellulose-based materials for skin tissue repair. *Carbohyd. Polym.* **2013**, *92*, 1432–1442. [CrossRef] [PubMed]
2. Cheng, F.; Liu, C.; Wei, X.; Yan, T.; Li, H.; He, J.; Huang, Y. Preparation and Characterization of 2,2,6,6-Tetramethylpiperidine-1-oxyl (TEMPO)-Oxidized Cellulose Nanocrystal/Alginate Biodegradable Composite Dressing for Hemostasis Applications. ACS Sustain. *Chem. Eng.* **2017**, *5*, 3819–3828.
3. Wang, Y.; Nie, J.; Fang, W.; Yang, L.; Hu, Q.; Wang, Z.; Sun, J.Z.; Tang, B.Z. Sugar-Based Aggregation-Induced emission luminogens: Design, structures, and applications. *Chem. Rev.* **2020**, *120*, 4534–4577. [CrossRef]
4. Nie, J.; Pei, B.; Wang, Z.; Hu, Q. Construction of ordered structure in polysaccharide hydrogel: A review. *Carbohydr. Polym.* **2019**, *205*, 225–235. [CrossRef]
5. Pei, B.; Wang, Z.; Nie, J.; Hu, Q. Highly mineralized chitosan-based material with large size, gradient mineral distribution and hierarchical structure. *Carbohydr. Polym.* **2019**, *208*, 336–344. [CrossRef]
6. Chen, E.; Yang, L.; Ye, C.; Zhang, W.; Ran, J.; Xue, D.; Wang, Z.; Pan, Z.; Hu, Q. An asymmetric chitosan scaffold for tendon tissue engineering: In vitro and in vivo evaluation with rat tendon stem/progenitor cells. *Acta Biomater.* **2018**, *73*, 377–387. [CrossRef]
7. Huang, X.; Sun, Y.; Nie, J.; Lu, W.; Yang, L.; Zhang, Z.; Yin, H.; Wang, Z.; Hu, Q. Using absorbable chitosan hemostatic sponges as a promising surgical dressing. *Int. J. Biol. Macromol.* **2015**, *75*, 322–329. [CrossRef]
8. Qiao, F.; Ke, J.; Liu, Y.; Pei, B.; Hu, Q.; Tang, B.Z.; Wang, Z. Cationic quaternized chitosan bioconjugates with aggregation-induced emission features for cell imaging. *Carbohydr. Polym.* **2020**, *230*, 115614. [CrossRef]
9. Yang, L.; Lu, W.; Pang, Y.; Huang, X.; Wang, Z.; Qin, A.; Hu, Q. Fabrication of a novel chitosan scaffold with asymmetric structure for guided tissue regeneration. *RSC Adv.* **2016**, *6*, 71567–71573. [CrossRef]
10. Jin, X.; Jiang, H.; Li, G.; Fu, B.; Bao, X.; Wang, Z.; Hu, Q. Stretchable, conductive PAni-PAAm-GOCS hydrogels with excellent mechanical strength, strain sensitivity and skin affinity. *Chem. Eng. J.* **2020**, *394*, 124901. [CrossRef]

11. Feng, W.; Wang, Z. Biomedical applications of chitosan-graphene oxide nanocomposites. *iScience* **2022**, *25*, 103629. [CrossRef]
12. Liu, X.; Wu, Y.; Zhao, X.; Wang, Z. Fabrication and applications of bioactive chitosan-based organic-inorganic hybrid materials: A review. *Carbohydr. Polym.* **2021**, *267*, 118179. [CrossRef] [PubMed]
13. Huang, X.; Bao, X.; Liu, Y.; Wang, Z.; Hu, Q. Catechol-Functional Chitosan/Silver nanoparticle composite as a highly effective antibacterial agent with Species-Specific mechanisms. *Sci. Rep.* **2017**, *7*, 1860. [CrossRef]
14. Koumentakou, I.; Terzopoulou, Z.; Michopoulou, A.; Kalafatakis, I.; Theodorakis, K.; Tzetzis, D.; Bikiaris, D. Chitosan dressings containing inorganic additives and levofloxacin as potential wound care products with enhanced hemostatic properties. *Int. J. Biol. Macromol.* **2020**, *162*, 693–703. [CrossRef] [PubMed]
15. Yang, S.; Miao, Q.; Huang, Y.; Jian, P.; Wang, X.; Tu, M. Preparation of cinnamaldehyde-loaded polyhydroxyalkanoate/chitosan porous microspheres with adjustable controlled-release property and its application in fruit preservation. *Food Packag. Shelf Life* **2020**, *26*, 100596. [CrossRef]
16. Sun, X.; Wu, Q.; Picha, D.H.; Ferguson, M.H.; Ndukwe, I.E.; Azadi, P. Comparative performance of bio-based coatings formulated with cellulose, chitin, and chitosan nanomaterials suitable for fruit preservation. *Carbohyd. Polym.* **2021**, *259*, 117764. [CrossRef]
17. Kim, J.; Kim, T.H.; Lee, J.H.; Park, Y.A.; Kang, Y.J.; Ji, H.G. Porous nanocomposite of layered double hydroxide nanosheet and chitosan biopolymer for cosmetic carrier application. *Appl. Clay Sci.* **2021**, *205*, 106067. [CrossRef]
18. Chen, K.; Guo, B.; Luo, J. Quaternized carboxymethyl chitosan/organic montmorillonite nanocomposite as a novel cosmetic ingredient against skin aging. *Carbohyd. Polym.* **2017**, *173*, 100–106. [CrossRef]
19. Bikiaris, N.D.; Michailidou, G.; Lazaridou, M.; Christodoulou, E.; Gounari, E.; Ofrydopoulou, A.; Lambropoulou, D.A.; Vergkizi-Nikolakaki, S.; Lykidou, S.; Nikolaidis, N. Innovative skin product emulsions with enhanced antioxidant, antimicrobial and UV protection properties containing nanoparticles of pure and modified chitosan with encapsulated fresh pomegranate juice. *Polymers* **2020**, *12*, 1542. [CrossRef]
20. Li, W.; Wei, H.; Liu, Y.; Li, S.; Wang, G.; Guo, T.; Han, H. An in situ reactive spray-drying strategy for facile preparation of starch-chitosan based hydrogel microspheres for water treatment application. *Chem. Eng. Process.-Process Intensif.* **2021**, *168*, 108548. [CrossRef]
21. El-Shafai, N.M.; Shawky, S.; El-Mehasseb, I.M.; El-Kemary, M.A. Sandwich nanohybrid of chitosan-polyvinyl alcohol for water treatment and Sofosbuvir drug delivery for anti-hepatitis C virus (HCV). *Int. J. Biol. Macromol.* **2021**, *190*, 927–939. [CrossRef] [PubMed]
22. Jin, E.; Wang, Z.; Li, M.; Hu, Q.; Tang, B.Z.; Yuan, J. Fluorescent sizing agents based on Aggregation-Induced emission effect for accurate evaluation of permeability and coating property. *Fiber. Polym.* **2021**, *22*, 1218–1227. [CrossRef]
23. Jin, E.; Wang, Z.; Hu, Q.; Li, M.; Yuan, J. Perylene-Based fluorescent sizing agent for precise evaluation of permeability and coating property of sizing paste. *Adv. Fiber Mater.* **2020**, *2*, 279–290. [CrossRef]
24. Lim, C.; Lee, D.W.; Israelachvili, J.N.; Jho, Y.; Hwang, D.S. Contact time- and pH-dependent adhesion and cohesion of low molecular weight chitosan coated surfaces. *Carbohyd. Polym.* **2015**, *117*, 887–894. [CrossRef]
25. Wang, W.; Xue, C.; Mao, X. Chitosan: Structural modification, biological activity and application. *Int. J. Biol. Macromol.* **2020**, *164*, 4532–4546. [CrossRef]
26. Du, X.; Wu, L.; Yan, H.; Jiang, Z.; Li, S.; Li, W.; Bai, Y.; Wang, H.; Cheng, Z.; Kong, D.; et al. Microchannelled alkylated chitosan sponge to treat noncompressible hemorrhages and facilitate wound healing. *Nat. Commun.* **2021**, *12*, 4733. [CrossRef]
27. Mourya, V.K.; Inamdara, N.; Ashutosh Tiwari, N. Carboxymethyl chitosan and its applications. *Adv. Mater. Lett.* **2010**, *1*, 11–33. [CrossRef]
28. Andreica, B.; Cheng, X.; Marin, L. Quaternary ammonium salts of chitosan. A critical overview on the synthesis and properties generated by quaternization. *Eur. Polym. J.* **2020**, *139*, 110016. [CrossRef]
29. Liu, W.; Sun, S.; Cheng, N. Preparation of Temperature-Sensitive Chitosan-Graft-NIPAAm/VL Copolymer Transgenic Carrier. China Patent CN 20041072351, 21 October 2004.
30. Chen, Z.; Yao, X.; Liu, L.; Guan, J.; Liu, M.; Li, Z.; Yang, J.; Huang, S.; Wu, J.; Tian, F.; et al. Blood coagulation evaluation of N -alkylated chitosan. *Carbohyd. Polym.* **2017**, *173*, 259–268. [CrossRef]
31. Petit, C.; Reynaud, S.; Desbrieres, J. Amphiphilic derivatives of chitosan using microwave irradiation. Toward an eco-friendly process to chitosan derivatives. *Carbohyd. Polym.* **2015**, *116*, 26–33.
32. Wang, Z.; Nie, J.; Qin, W.; Hu, Q.; Tang, B.Z. Gelation process visualized by aggregation-induced emission fluorogens. *Nat. Commun.* **2016**, *7*, 12033. [CrossRef]
33. Nie, J.; Wang, Z.; Hu, Q. Difference between Chitosan Hydrogels via Alkaline and Acidic Solvent Systems. *Sci. Rep.* **2016**, *6*, 36053. [CrossRef] [PubMed]
34. Nie, J.; Wang, Z.; Zhang, J.; Yang, L.; Pang, Y.; Hu, Q. High strength chitosan rod prepared via LiOH/urea solvent through centrifugation induced orientation processing. *RSC Adv.* **2015**, *5*, 66825–68243. [CrossRef]
35. Almeida, E.V.R.; Frollini, E.; Castellan, A.; Coma, V. Chitosan, sisal cellulose, and biocomposite chitosan/sisal cellulose films prepared from thiourea/NaOH aqueous solution. *Carbohyd. Polym.* **2010**, *80*, 655–664. [CrossRef]
36. Bi, S.; Hu, S.; Zhou, Z.; Kong, M.; Liu, Y.; Feng, C.; Cheng, X.; Chen, X. The green and stable dissolving system based on KOH/urea for homogeneous chemical modification of chitosan. *Int. J. Biol. Macromol.* **2018**, *120*, 1103–1110. [CrossRef]
37. Sun, X.; Li, J.; Shao, K.; Su, C.; Bi, S.; Mu, Y.; Zhang, K.; Cao, Z.; Wang, X.; Chen, X.; et al. A composite sponge based on alkylated chitosan and diatom-biosilica for rapid hemostasis. *Int. J. Biol. Macromol.* **2021**, *182*, 2097–2107. [CrossRef]

38. Pei, L.; Cai, Z.; Shang, S.; Song, Z. Synthesis and antibacterial activity of alkylated chitosan under basic ionic liquid conditions. *J. Appl. Polym. Sci.* **2014**, *131*. [CrossRef]
39. Le Tien, C.; Lacroix, M.; Ispas-Szabo, P.; Mateescu, M. N-acylated chitosan: Hydrophobic matrices for controlled drug release. *J. Control Release* **2003**, *93*, 1–13. [CrossRef]
40. Rodrigues, M.R. Synthesis and investigation of chitosan derivatives formed by reaction with acyl chlorides. *J. Carbohyd. Chem.* **2005**, *24*, 41–54. [CrossRef]
41. Hu, Y.; Du, Y.; Yang, J.; Tang, Y.; Li, J.; Wang, X. Self-aggregation and antibacterial activity of N-acylated chitosan. *Polymer* **2007**, *48*, 3098–3106. [CrossRef]
42. Zhen, Z.; Fujun, J.; Zicong, W.; Ju, J.; Feng, L.; Yiliang, W.; Zhiping, W.; Shunqing, T.; Chaoxi, W.; Yifei, W. O-acylation of chitosan nanofibers by short-chain and long-chain fatty acids. *Carbohyd. Polym.* **2017**, *177*, 203–209.
43. Wang, X.; Dang, Q.; Liu, C.; Chang, G.; Song, H.; Xu, Q.; Ma, Y.; Li, B.; Zhang, B.; Cha, D. Antibacterial porous sponge fabricated with capric acid-grafted chitosan and oxidized dextran as a novel hemostatic dressing. *Carbohyd. Polym.* **2022**, *277*, 118782. [CrossRef] [PubMed]
44. Liu, M.; Yang, J.; Guan, J.; Huang, S.; Li, Z.; Jing, M. Effect of grafted chain length on hemostatic activity of N-Alkylated chitosan. In Proceedings of the 4th Annual International Conference on Material Engineering and Application (ICMEA 2017), Wuhan, China, 15–17 December 2017; Volume 146, pp. 229–234.
45. Huang, Y.; Feng, L.; Zhang, Y.; He, L.; Wang, C.; Xu, J.; Wu, J.; Kirk, T.B.; Guo, R.; Xue, W. Hemostasis mechanism and applications of N-alkylated chitosan sponge. *Polym. Advan. Technol.* **2017**, *28*, 1107–1114. [CrossRef]
46. Huang, Y.; Zhang, Y.; Feng, L.; He, L.; Guo, R.; Xue, W. Synthesis of N-alkylated chitosan and its interactions with blood. *Artif. Cells Nanomed. Biotechnol.* **2018**, *46*, 544–550. [CrossRef]
47. Wang, X.; Guan, J.; Zhuang, X.; Li, Z.; Huang, S.; Yang, J.; Liu, C.; Li, F.; Tian, F.; Wu, J.; et al. Exploration of blood coagulation of N-Alkyl chitosan nanofiber membrane in vitro. *Biomacromolecules* **2018**, *19*, 731–739. [CrossRef]
48. Dowling, M.B.; Kumar, R.; Keibler, M.A.; Hess, J.R.; Bochicchio, G.V.; Raghavan, S.R. A self-assembling hydrophobically modified chitosan capable of reversible hemostatic action. *Biomaterials* **2011**, *32*, 3351–3357. [CrossRef] [PubMed]
49. Dowling, M.B.; Smith, W.; Balogh, P.; Duggan, M.J.; Macintire, I.C.; Harris, E.; Mesar, T.; Raghavan, S.R.; King, D.R. Hydrophobically-modified chitosan foam: Description and hemostatic efficacy. *J. Surg. Res.* **2015**, *193*, 316–323. [CrossRef] [PubMed]
50. Logun, M.T.; Dowling, M.B.; Raghavan, S.R.; Wallace, M.L.; Schmiedt, C.; Stice, S.; Karumbaiah, L. Expanding hydrophobically modified chitosan foam for internal surgical hemostasis: Safety evaluation in a murine model. *J. Surg. Res.* **2019**, *239*, 269–277.
51. Chaturvedi, A.; Dowling, M.B.; Gustin, J.P.; Scalea, T.M.; Raghavan, S.R.; Pasley, J.D.; Narayan, M. Hydrophobically modified chitosan gauze: A novel topical hemostat. *J. Surg. Res.* **2017**, *207*, 45–52. [CrossRef]
52. Chen, Z.; Han, L.; Liu, C.; Du, Y.; Hu, X.; Du, G.; Shan, C.; Yang, K.; Wang, C.; Li, M.; et al. A rapid hemostatic sponge based on large, mesoporous silica nanoparticles and N-alkylated chitosan. *Nanoscale* **2018**, *10*, 20234–20245. [CrossRef]
53. Zhang, Y.; Guan, J.; Wu, J.; Ding, S.; Yang, J.; Zhang, J.; Dong, A.; Deng, L. N-alkylated chitosan/graphene oxide porous sponge for rapid and effective hemostasis in emergency situations. *Carbohyd. Polym.* **2019**, *219*, 405–413. [CrossRef] [PubMed]